

Supplementary Information

Contents

- Figure S1. Yearly domestic *P. vivax* malaria cases in 2009–2018.
- Figure S2. Weekly *P. vivax* malaria cases in 2014–2018 based on the data and model prediction with the estimated parameters.
- Model equations
- Table S1. Descriptions, values, and references for the model parameters.
- Results obtained from HIRA data
 - Table S2. Average expenditure (USD) of medical use, benefits, and costs for one patient in 2019 estimated from HIRA data.
 - Table S3. Yearly total medical costs and cumulative costs over 10 years.
 - Figure S3. Yearly cumulative incremental benefits and costs and IBCRs, 2019–2028.
- Figure S4. Scatter plot of incremental costs and incremental benefits in 2028.
- References

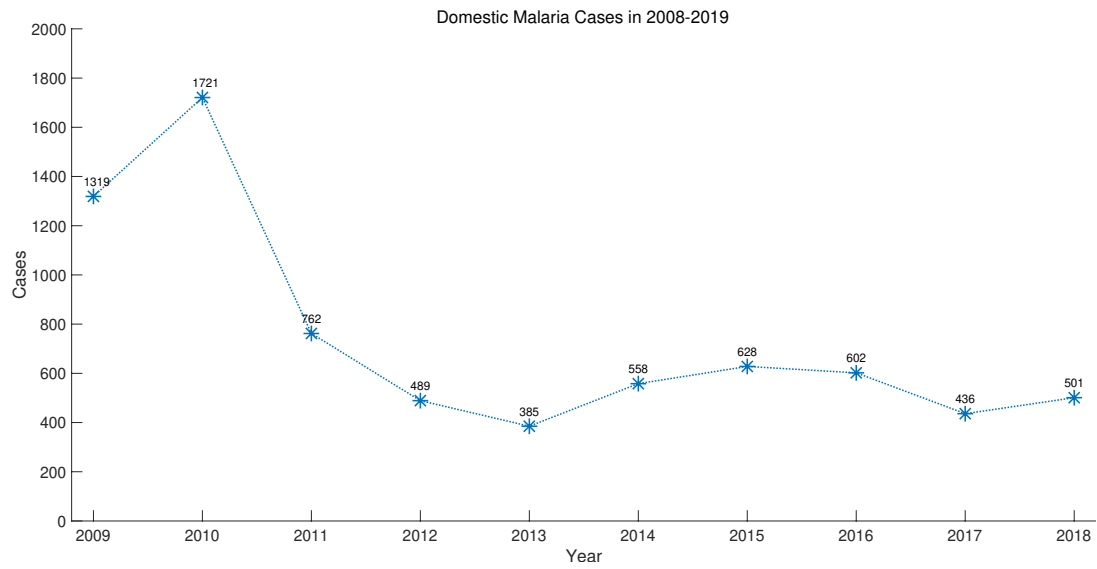
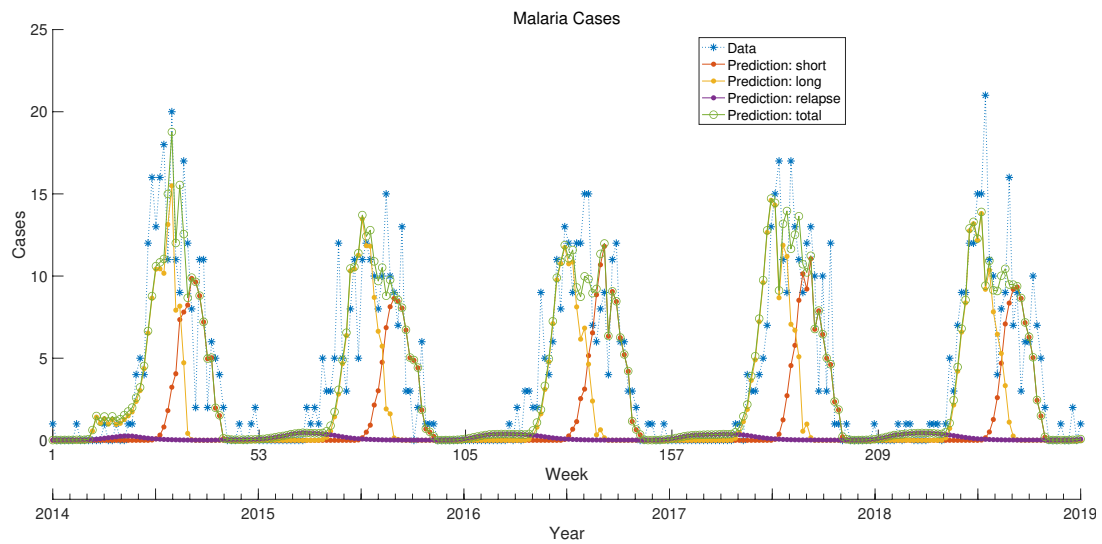
Figure S1. Yearly domestic *P. vivax* malaria cases in 2009-2018.

Figure S2. Weekly *P. vivax* malaria cases in 2014-2018 based on the data and model prediction with the estimated parameters. The total number of cases is the sum of short, long, and relapse cases.



Model equations

The model is described by delay differential equations (DDEs). Delays are added to the exposed state (E_h) for the implementation of different latency periods. There are three latency periods: short, long, and relapse.

$$\frac{dS_h(t)}{dt} = \mu_h N_h(t) - \lambda_h(t) S_h(t) + (1 - q) \rho_h T_h(t) - \delta_h S_h(t)$$

$$\begin{aligned} \frac{dE_h(t)}{dt} = & \lambda_h(t) S_h(t) - p \lambda_h(t - \tau_s) S_h(t - \tau_s) e^{-\delta_h \tau_s} - (1 - p) \lambda_h(t - \tau_l) S_h(t - \tau_l) e^{-\delta_h \tau_l} + q \rho_h T_h(t) \\ & - q \rho_h T_h(t - \tau_r) e^{-\delta_h \tau_r} - \delta_h E_h(t) \end{aligned}$$

$$\begin{aligned} \frac{dI_h(t)}{dt} = & p \lambda_h(t - \tau_s) S_h(t - \tau_s) e^{-\delta_h \tau_s} + (1 - p) \lambda_h(t - \tau_l) S_h(t - \tau_l) e^{-\delta_h \tau_l} + q \rho_h T_h(t - \tau_r) e^{-\delta_h \tau_r} - \gamma_h I_h(t) \\ & - \delta_h I_h(t) \end{aligned}$$

$$\frac{dT_h(t)}{dt} = \gamma_h I_h(t) - \rho_h T_h(t) - \delta_h T_h(t)$$

$$\frac{dA(t)}{dt} = \mu_a(t) \left(1 - \frac{A(t)}{k_a} \right) N_v(t) - \mu_v(t) A(t) - \delta_a(t) A(t)$$

$$\frac{dS_v(t)}{dt} = \mu_v(t) A(t) - \lambda_v(t) S_v(t) - \delta_v(t) S_v(t)$$

$$\frac{dE_v(t)}{dt} = \lambda_v(t) S_v(t) - \nu_v E_v(t) - \delta_v(t) E_v(t)$$

$$\frac{dI_v(t)}{dt} = \nu_v E_v(t) - \delta_v(t) I_v(t)$$

where the force of infections are $\lambda_h(t) = b(t) \beta_{hv} \frac{I_v}{N_h}$ for humans, $\lambda_v(t) = b(t) \beta_{vh} \frac{I_h}{N_h}$ for mosquitoes, and the total number of humans $N_h(t) = S_h(t) + E_h(t) + I_h(t) + T_h(t)$, and the total number of adult mosquitoes $N_v(t) = S_v(t) + E_v(t) + I_v(t)$.

Table S1. Descriptions, values, and references for the model parameters. * temperature-dependent parameters.

Parameter	Description	Value	Reference
Human			
μ_h	Birth rate of humans	0.0081	[1]
δ_h	Death rate of humans	0.0052	[1]
p	Probability of having short latency period	0.4295	Estimated
τ_s	Average short latency period	14 days	[2]
τ_l	Average long latency period	314 days	[2]
τ_r	Average latency period for relapse	207 days	[2]
γ_h	Treatment starting rate = 1/Average infectious period	1/41 days	[2]
ρ_h	Recovery rate = 1/Average duration of drug action	1/351 days	[3]
q	Probability of relapse	0.04	[2, 4]
Mosquito			
k_a	Vector carrying capacity	165 × N_h	[5, 6]
μ_a^*	Egg deposition rate per adult mosquito $\max\{-0.153T^2 + 8.61T - 97.7, 0\}$ T : temperature(°C)		[5-7]
δ_a^*	Death rate of immature mosquitoes $\min\left\{0.002 \exp\left(\left(\frac{T-23}{6.05}\right)^2\right), 1\right\}$		[5, 6, 8]
μ_v^*	Maturation rate $\begin{cases} \frac{e(T)p_E(R)p_L(T,R)p_P(R)}{\tau_{EA}(T)} & 16.5 \leq T \leq 35.6 \\ 0 & \text{otherwise} \end{cases}$ • $e(T) = \frac{f(T)}{\delta_v(T)}$: Lifetime number of eggs laid by adult mosquitoes.		[5, 6, 9]

	<ul style="list-style-type: none"> • $f(T) = -0.153T^2 + 8.61T - 97.7$: Total number of eggs laid per day. • $1/\delta_v(T)$: Average adult mosquito lifespan. • $p_E(R) = \frac{3.6(R_L - R)}{R_L^2}$: Daily survival probability of eggs. R and R_L denote rainfall (mm) and rainfall threshold (mm), and fixed to 3mm and 76mm, respectively. • $p_L(T, R) = \exp\{-0.00554T + 0.06737\} \frac{R(R_L - R)}{R_L^2}$: Daily survival probability of larvae. • $p_P(R) = \frac{3R(R_L - R)}{R_L^2}$: Daily survival probability of pupae. • $\tau_{EA}(T) = 1/(-0.00094T^2 + 0.049T - 0.552)$: Total development time from egg to adult mosquito. 		
δ_v^*	Death rate of adult mosquitoes $\begin{cases} 1 & T \leq -4 \\ -\frac{29}{570}T + \frac{227}{259} & -4 < T \leq 15 \\ \frac{1}{30} & 15 < T \leq 32 \\ \frac{29}{570}T - \frac{303}{190} & 32 < T \end{cases}$		[2, 5-7]
ν_v	Progression rate of mosquitoes to the infectious state = 1/Average latency period of mosquitoes	1/10 1/day	[2, 10]
Transmission			
λ_h^*	Force of infection from mosquitoes to humans $\lambda_h(T) = b_h(T)\beta_{hv} \frac{I_v}{N_v} = b(T)\beta_{hv} \frac{I_v}{N_h}$		[11]
λ_v^*	Force of infection from humans to mosquitoes $\lambda_v(T) = b_v(T)\beta_{vh} \frac{I_h}{N_h} = b(T)\beta_{vh} \frac{I_h}{N_h}$		[11]
b_h^*	Biting rate for humans is defined as the number of mosquito bites per human per unit time $b_h(T) = b(T) \times \frac{N_v}{N_h}$ $= \begin{cases} 0 & T < 0 \\ 0.000203T(T - 11.7)\sqrt{42.3 - T} \times \frac{N_v}{N_h} & T \geq 0 \end{cases}$		[5-7, 11]
b_v^*	Biting rate for mosquitoes refers to the number of human bites for one mosquito per unit time $b_h(T) = b(T)$ $= \begin{cases} 0 & T < 0 \\ 0.000203T(T - 11.7)\sqrt{42.3 - T} & T \geq 0 \end{cases}$		[5-7, 11]
β_{hv}	Probability of transmission of infection from an infectious mosquito to a susceptible human	0.09 79	Estimated
β_{vh}	Probability of transmission of infection from an infectious human to	0.03	Estimated

	a susceptible mosquito	55	ed
--	------------------------	----	----

Results obtained from HIRA data

We also explored the monetary influences of RDT introduction on medical costs estimated from the HIRA data as a nationally representative database. As the cost extraction structure in the HIRA is not completely consistent with that in the NHIIH, the estimated average medical costs were smaller than those of the NHIIH, while the difference between the two medical costs increased, leading to a smaller benefit for RDTs as shown in Table S2. Therefore, the resulting IBCR value is the repetition of the sensitivity analysis in the main text, but we can verify how this value is derived.

	Microscopy only	Microscopy + RDT
Medical costs (\$)	583.39	593.30
Benefits (\$)	0	12.98
Costs (\$)	11.72	35.63

Table S2. Average expenditure (USD) of medical use, benefits, and costs for one patient in 2019 estimated from HIRA data.

Despite the lower benefit, total medical costs were saved for 10 consecutive years as shown in Table S3 because of the reduced malaria incidence in the microscopy + RDT scenario. In Figure S3, the trend of IBCRs is the same as the results described in the main text; however, in this case, beneficial results can be seen from the ninth year. Hence, the lower the benefit, the more the years of continuous RDT implementation required.

Year	Yearly costs (\$)				Yearly cumulative costs (\$)			
	Microscopy only	Microscopy + RDT	Saved		Microscopy only	Microscopy + RDT	Saved	
2019	107,435	101,751	5,684	5.3%	107,435	101,751	5,684	5.3%
2020	105,920	83,541	22,379	21.1%	213,355	185,292	28,063	13.2%
2021	102,495	66,007	36,488	35.6%	315,850	251,299	64,551	20.4%
2022	100,026	52,546	47,480	47.5%	415,876	303,845	112,031	26.9%
2023	97,384	41,745	55,639	57.1%	513,260	345,590	167,670	32.7%
2024	94,428	32,948	61,480	65.1%	607,688	378,538	229,150	37.7%
2025	91,209	25,865	65,344	71.6%	698,897	404,403	294,494	42.1%
2026	87,660	20,222	67,438	76.9%	786,557	424,625	361,932	46.0%
2027	83,871	15,750	68,121	81.2%	870,428	440,375	430,053	49.4%
2028	79,893	12,227	67,666	84.7%	950,321	452,602	497,719	52.4%

Table S3. Yearly total medical costs and cumulative costs over 10 years.

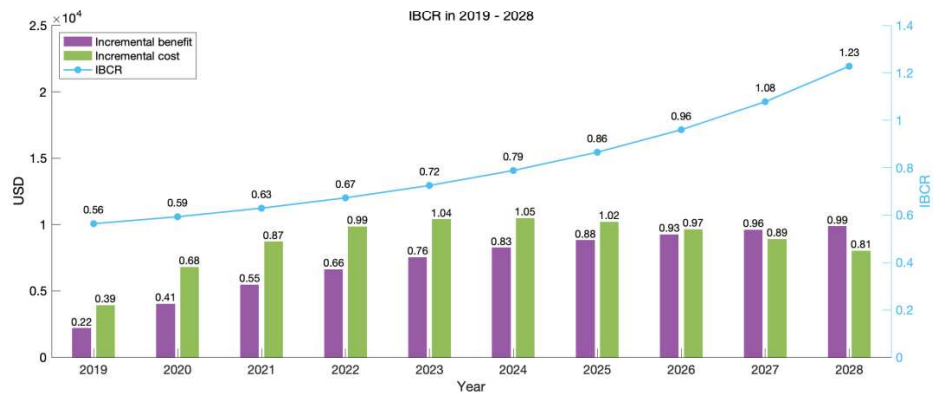


Figure S3. Yearly cumulative incremental benefits and costs and IBCRs, 2019-2028.

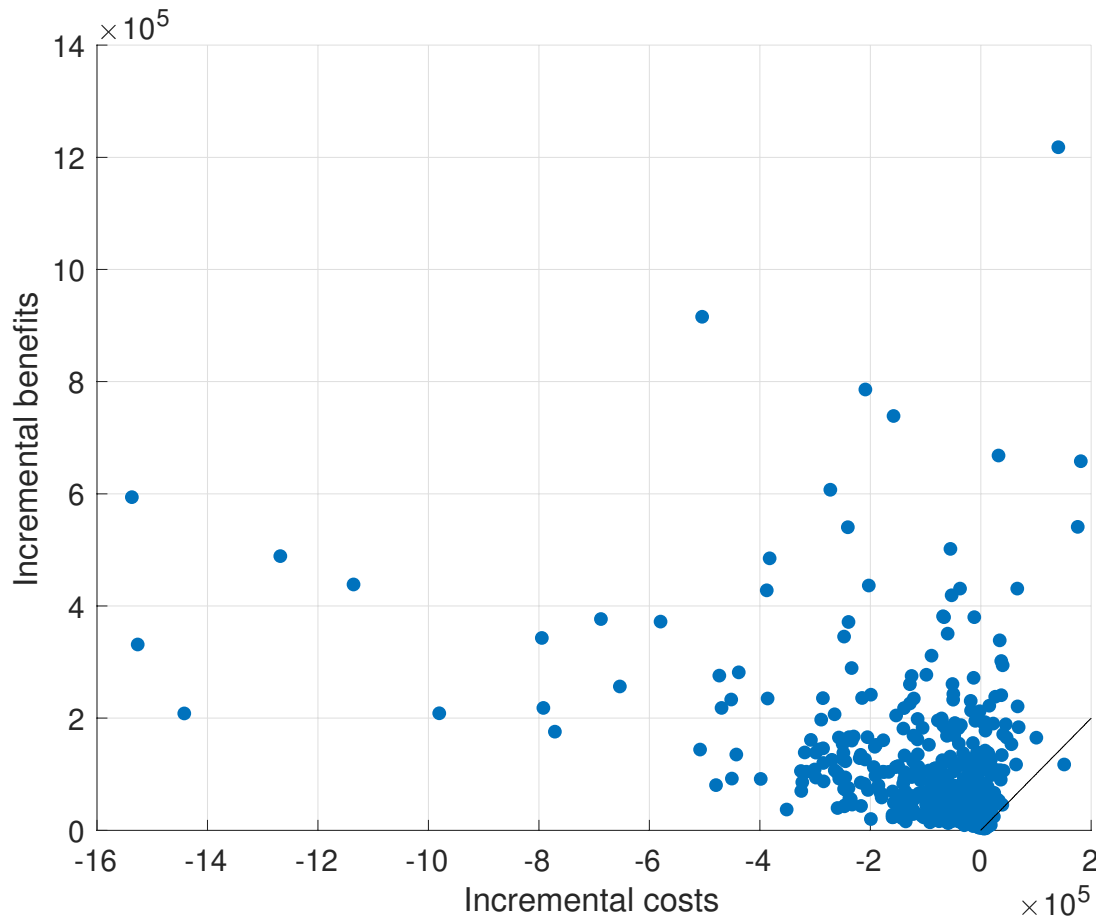


Figure S4. Scatter plot of incremental costs and incremental benefits in 2028. Solid line indicates IBCR = 1.

References

- [1] Korean Statistical Information Service. Birth and death rates per 1,000 by region.
- [2] Korea Centers for Disease Control and Prevention. Malaria management guidelines 2018 (2018).
- [3] Baird, J. K. Chloroquine resistance in plasmodium vivax. *Antimicrob. agents and chemotherapy* **48**, 4075–4083 (2004).
- [4] Chu, C. S. & White, N. J. Management of relapsing plasmodium vivax malaria. *Expert. review anti-infective therapy* **14**, 885–900 (2016).
- [5] Kim, J. E., Choi, Y. & Lee, C. H. Effects of climate change on plasmodium vivax malaria transmission dynamics: A mathematical modeling approach. *Appl. Math. Comput.* **347**, 616–630 (2019).
- [6] Korea Meteorological Administration. Daily temperature and rainfall in 2013–2018.
- [7] Mordecai, E. A. et al. Optimal temperature for malaria transmission is dramatically lower than previously predicted. *Ecol. Letters* **16**, 22–30 (2013).
- [8] Beck-Johnson, L. M. et al. The effect of temperature on anopheles mosquito population dynamics and the potential for malaria transmission. *PLOS one* **8**, e79276 (2013).
- [9] Okuneye, K. & Gumel, A. B. Analysis of a temperature-and rainfall-dependent model for malaria transmission dynamics. *Math. Biosciences* **287**, 72–92 (2017).
- [10] Mandal, S., Sarkar, R. R. & Sinha, S. Mathematical models of malaria-a review. *Malar. Journal* **10**, 1–19 (2011).
- [11] Chitnis, N., Cushing, J. M. & Hyman, J. Bifurcation analysis of a mathematical model for malaria transmission. *SIAM J. on Appl. Math.* **67**, 24–45 (2006).